Stochastic seismic response of base-isolated buildings

Article *in* International Journal of Applied Mechanics · March 2013

DOI: 10.1142/S1758825113500063

4 authors, including:

Cibi Jacob

1 PUBLICATION **5** CITATIONS

SEE PROFILE

Vasant Matsagar

Indian Institute of Technology Delhi

113 PUBLICATIONS **453** CITATIONS

SEE PROFILE

Steffen Marburg

Technische Universität München

193 PUBLICATIONS **1,642** CITATIONS

SEE PROFILE

International Journal of Applied Mechanics
Vol. 5, No. 1 (2013) 1350006 (21 pages)

DOI: 10.1142/S1758825113500063

ICP Imperial College Press
www.icpress.co.uk

STOCHASTIC SEISMIC RESPONSE OF BASE-ISOLATED BUILDINGS

C. JACOB*, K. SEPAHVAND†,‡, V. A. MATSAGAR*
and S. MARBURG†

*Department of Civil Engineering
Indian Institute of Technology Delhi
New Delhi, India

†Institute of Mechanics, Universität der Bundeswehr
Munich, Germany
‡sepahvand@unibw.de

Received 4 August 2012
Accepted 21 December 2012
Published 29 March 2013

The stochastic response of base-isolated building considering the uncertainty in the characteristics of the earthquakes is investigated. For this purpose, a probabilistic ground motion model, for generating artificial earthquakes is developed. The model is based upon a stochastic ground motion model which has separable amplitude and spectral non-stationarities. An extensive database of recorded earthquake ground motions is created. The set of parameters required by the stochastic ground motion model to depict a particular ground motion is evaluated for all the ground motions in the database. Probability distributions are created for all the parameters. Using Monte Carlo (MC) simulations, the set of parameters required by the stochastic ground motion model to simulate ground motions is obtained from the distributions and ground motions. Further, the bilinear model of the isolator described by its characteristic strength, post-yield stiffness and yield displacement is used, and the stochastic response is determined by using an ensemble of generated earthquakes. A parametric study is conducted for the various characteristics of the isolator. This study presents an approach for stochastic seismic response analysis of base-isolated building considering the uncertainty involved in the earthquake ground motion.

Keywords: Base isolation; stochastic response; ground motion model; artificial earthquakes; bilinear model.

1. Introduction

Ground motion at a particular site due to earthquakes is influenced by source, travel path and local site conditions. It is well known that earthquake ground motions are non-stationary in both time and frequency domains [Fan and Ahmadi, 1990]. Amplitude non-stationarity refers to the variation in the intensity of the ground

‡Corresponding author.

motion in time. Spectral non-stationarity refers to the variation in the frequency content of the motion in time.

There are two types of stochastic ground motion models: models that describe the random occurrence of fault ruptures at the source and propagation of the resulting seismic waves through the ground medium (source-based models) [Zerva, 1988], and models that describe the ground motion for a specific site by fitting to a recorded motion with known earthquake and site characteristics (site-based models). By using a site-based stochastic model, artificial ground motions can be generated, which have statistical characteristics similar to those of the target ground motion. A large number of site-based models have been proposed in the past [Shinozuka and Deodatis, 1988; Kiureghian and Crempien, 1989; Conte and Peng, 1997]. A fully non-stationary stochastic model for strong earthquake ground motion was developed by Rezaeian and Kiureghian [2008]. The model employs filtering of a discretized white-noise process. Non-stationarity is achieved by modulating the intensity and varying the filter properties in time. Previous studies [Schueller *et al.*, 1988; Su and Ahmadi, 1988; Constantinou and Papageorgiou, 1990; Yeh and Wen, 1990; Er and Iu, 2000; Alhan and Gavin, 2005] have demonstrated that Monte Carlo (MC) simulation is an effective method in obtaining stochastic response statistics. Studies show that the results have a reasonable agreement with the analytical solutions. Albeit it is not as accurate and time efficient as other approaches such as generalized polynomial chaos expansion [Sepahvand *et al.*, 2011], the MC simulation is still a convenient method for calculating the probability of failure.

One of the emerging tools for protecting structures from the damaging effects of earthquakes is the use of base isolation systems. Seismic isolation is achieved by inserting flexible isolators which shift the vibration period and increase energy dissipation. In base isolation, isolators or base isolation systems decouple the superstructure from shaking the ground in horizontal direction. The isolators possess high axial and low horizontal stiffness so that along with lateral flexibility, the vertical loads are effectively carried to the ground. Due to the decoupling, inter-storey deformations and floor acceleration are minimized. Thus, base isolation enables a building or non-building structure to survive a potentially devastating seismic event. Various types of isolation systems have been used in structures and well documented in the literature [Kelly, 1986; Buckle and Mayes, 1990; Jangid and Datta, 1995; Ibrahim, 2008]. Although uncertainty in structural parameters with linearity [Jensen and Iwan, 1992] and nonlinearity [Jensen *et al.*, 2012] such as the base-isolated building has been considered, the uncertainty in earthquake excitation still needs a detailed investigation. With this aim, the stochastic response of a base-isolated building under earthquake excitations with emphasis on the uncertainty in the earthquake loading is presented here.

The objectives of the present study are to: (i) create a database of earthquakes and fit all the earthquakes to a stochastic ground motion model; (ii) determine the probability density function of all the parameters required to generate an artificial

ground motion of required statistical characteristics; and (iii) generate a large number of artificial ground motions and perform stochastic response analysis and parametric studies for a base-isolated building.

2. Analytical Model of Stochastic Ground Motion

A fully analytical model for non-stationary stochastic ground motion proposed by Rezaeian and Kiureghian [2008] in which filtering of a discretized white-noise process is employed. Non-stationarity is achieved by modulating the intensity and varying the filter properties in time. The stochastic ground motion model selected considers both the amplitude and spectral non-stationarities. The equations and the procedure to calculate the ground acceleration, $\hat{x}(t)$ at any time t are described here [Rezaeian and Kiureghian, 2008]

$$\hat{x}(t) = q(t) \sum_{i=1}^{k} s_i(t) u_i, \quad \text{for} \quad t_k \le t < t_{k+1}, \tag{1}$$

where $q(t)$ is the modulating function at time t and u_i is a standard random normal variable. A modified version of the Housner and Jennings [1964] model stated below is used as the modulating function

$$q(t) = \begin{cases} 0, & t \le T_0, \\ \sigma_{\max} \left(\dfrac{t - T_0}{T_1 - T_0} \right)^2, & T_0 < t \le T_1, \\ \sigma_{\max}, & T_1 \le t \le T_2, \\ \sigma_{\max} \exp[-\alpha (t - T_2)^{\beta}], & T_2 \le t. \end{cases} \tag{2}$$

This model has six parameters T_0, T_1, T_2, $\sigma_{\max}$, α and β which obey the conditions $T_0 < T_1 < T_2$, $0 < \sigma_{\max}$, $0 < \alpha$ and $0 < \beta$. Here, T_0 denotes the start time of the process, T_1 and T_2 denote the start and end times of the strong-motion phase with root mean square (RMS) $\sigma_{\max}$, and α and β are the parameters that shape the decaying end of the modulating function. In Housner and Jennings model β is taken as 1.

If $k = \text{int}(\frac{t}{\Delta t})$ where Δt is the time steps taken for discretizing the model, then

$$s_i(t) = \frac{h[t - t_i, \theta(t_i)]}{\sqrt{\sum_{j=1}^{k} h^2[t - t_j, \theta(t_j)]}}, \quad \text{for} \quad t_k \le t < t_{k+1}, \quad \text{and} \quad 0 < i \le k. \tag{3}$$

Any damped single- or multi-degree-of-freedom linear system that has differentiable response can be selected as the filter. Here

$$\begin{aligned} h[t - \tau, \theta(\tau)] &= \frac{\omega_f(\tau)}{\sqrt{1 - \zeta_f^2(\tau)}} \exp[-\zeta_f(\tau) \omega_f(\tau)(t - \tau)] \\ &\quad \times \sin[\omega_f(\tau) \sqrt{1 - \zeta_f^2(\tau)}(t - \tau)], \quad \text{for } \tau \le t, \\ h[t - \tau, \theta(\tau)] &= 0, \quad \text{otherwise}, \end{aligned} \tag{4}$$

represents the pseudo-acceleration response of a single-degree-of-freedom linear oscillator subjected to a unit impulse, in which τ denotes the time of the pulse. $\theta(\tau) = [\omega_f(\tau), \zeta_f(\tau)]$ is the set of parameters of the filter with $\omega_f(\tau)$ denoting the natural frequency and $\zeta_f(\tau)$ denoting the damping ratio, both dependent on the time of application of the pulse. $\omega_f(\tau)$ influences the predominant frequency of the resulting process, whereas $\zeta_f(\tau)$ influences its bandwidth. The predominant frequency of an earthquake ground motion tends to decay with time. Therefore,

$$\omega_f(\tau) = \omega_0 - (\omega_0 - \omega_n)\frac{\tau}{t_n}, \tag{5}$$

in which t_n is the total duration of the ground motion, ω_0 is the filter frequency at time $t_0 = 0$ and ω_n is the frequency at time t_n. For a typical ground motion, $\omega_n < \omega_0$. Thus, the two parameters ω_0 and ω_n describe the time-varying frequency content of the ground motion.

2.1. *Parameter identification*

As shown above, the amplitude and spectral characteristics of the proposed model are completely separable. Specifically, the modulating function $q(t)$ describes the evolving RMS amplitude of the process, whereas the filter Impulse Response Function (IRF) $h[t-\tau, \theta(\tau)]$ controls the evolving frequency content of the process. This means that the parameters of the modulating function and of the filter can be independently identified by matching to corresponding statistical characteristics of a target accelerogram.

2.1.1. *Identification of parameters in the modulating function*

Let $\boldsymbol{\alpha} = (T_0, T_1, T_2, \sigma_{\max}, \alpha, \beta)$ denote the parameters of the modulating function, so that $q(t) = q(t, \boldsymbol{\alpha})$. For a target accelerogram, $a(t)$, $\boldsymbol{\alpha}$ is determined by matching the expected cumulative energy of the process, $E_x(t) = (\frac{1}{2})\int_0^t q^2(\tau, \boldsymbol{\alpha})d\tau$, with the cumulative energy in the accelerogram, $E_a(t) = (\frac{1}{2})\int_0^t a^2(\tau)d\tau$, over the duration of the ground motion, $0 < t < t_n$. This is done by minimizing the integrated squared difference between the two cumulative energy terms, i.e.,

$$\tilde{\boldsymbol{\alpha}} = \underset{\alpha}{\operatorname{argmin}} \int_0^{t_n} \left(\frac{1}{2}\right) \left[\int_0^t q^2(\tau, \boldsymbol{\alpha})B(\tau)d\tau - \int_0^t a^2(\tau)B(\tau)d\tau\right]^2 \mathrm{d}t, \tag{6}$$

where $B(t)$ is a weight function introduced to avoid dominance by the strong-motion phase of the record (otherwise, the tail of the record is not well fitted). The function, $B(t) = \min\{[\max_t q_0^2(t)]/q_0^2(t), 5\}$, where $q_0(t)$ is the modulating function obtained in a prior optimization without the weight function. The objective function in Eq. (6), which was earlier used by Yeh and Wen [1990] without the weight function, has the advantage that the integral $\int_0^t a^2(\tau)B(\tau)\mathrm{d}\tau$ is a relatively smooth function so that no artificial smoothing is necessary.

2.1.2. *Identification of filter parameters*

The parameters ω_0 and ω_n defining the time-varying frequency of the filter, Eq. (5) and parameters defining its damping ratio $\zeta_f(\tau)$ control the predominant frequency and bandwidth of the process. Since these parameters have interacting influences, we first determine ω_0 and ω_n while keeping the filter damping a constant, ζ_f. For a given ζ_f, the parameters ω_0 and ω_n are identified by matching the cumulative expected number of zero-level up-crossings of the process, i.e., $\int_0^t \nu(0^+,\tau)\mathrm{d}\tau$, with the cumulative count $N(0^+,t)$ of zero-level up-crossings in the target accelerogram for all t, $0 < t < t_n$. This is accomplished by minimizing the mean-square error,

$$[\hat{\omega}_0(\zeta_f), \hat{\omega}_n(\zeta_f)] = \operatorname{argmin} \int_0^{t_n} \left(\frac{1}{2}\right) \left[\int_0^t \nu(0^+,\tau) r(\tau)\mathrm{d}\tau - N(0^+,t)\right]^2 \mathrm{d}t, \quad (7)$$

where $\nu(0^+,t)$ is the mean number of times per unit time that the process crosses the level zero from below is used and $r(\tau)$ is an adjustment factor. Since the scaling of a process does not affect its zero-level crossings, $\nu(0^+,t)$ for the process in Eq. (1) is identical to that for the process,

$$y(t) = \sum_{i=1}^{k} s_i(t) u_i, \quad \text{for} \quad t_k \le t < t_{k+1}. \quad (8)$$

It is known that for such a process,

$$\nu(0^+,t) = \frac{\sqrt{1-\rho_{y\dot{y}}^2(t)}}{2\pi} \frac{\sigma_{\dot{y}}(t)}{\sigma_y(t)}, \quad (9)$$

where $\sigma_y(t)$, $\sigma_{\dot{y}}(t)$ and $\rho_{y\dot{y}}^2(t)$ are the standard deviations and cross-correlation coefficient of $y(t)$ and its time derivative, $\dot{y}(t) = \mathrm{d}y(t)/\mathrm{d}t$ at time t. For the process in Eq. (8), these are given by:

$$\sigma_y^2(t) = \sum_{i=1}^{k} s_i^2(t) = 1, \quad \text{for } t_k \le t < t_{k+1}, \quad (10)$$

$$\sigma_y^2(t) = \sum_{i=1}^{k} \dot{s}_i^2(t), \quad \text{for } t_k \le t < t_{k+1}, \quad (11)$$

$$\rho_{y\dot{y}}(t) = \frac{1}{\sigma_{\dot{y}}(t)\sigma_y(t)} \sum_{i=1}^{k} s_i(t)\dot{s}_t(t), \quad \text{for } t_k \le t < t_{k+1}, \quad (12)$$

where $\dot{s}_i(t) = \mathrm{d}s_i(t)/\mathrm{d}t$. Using Eq. (3) and $h_i(t) = h[t - t_i, \theta(t_i)]$, it is shown that

$$\dot{s}_i(t) = \left[\dot{h}_i(t) - \frac{\sum_{j=1}^{k} h_j(t)\dot{h}_j(t)}{\sum_{j=1}^{k} h_j^2(t)} h_i(t)\right] \frac{1}{\sqrt{\sum_{j=1}^{k} h_j^2(t)}}, \quad \text{for} \quad t_k \le t < t_{k+1}, \quad \text{and} \quad 0 < i \le k, \quad (13)$$

where $\nu(0^+, \tau)$ is an implicit function of the filter characteristics $\omega_f(\tau)$ and $\zeta_f(\tau)$ and therefore, ω_0, ω_n and ζ_f; which is also true for $r(\tau)$. When a continuous-parameter stochastic process is represented as a sequence of discrete-time points of equal intervals Δt, the process effectively loses its content beyond a frequency approximately equal to $\pi/2\Delta t$ rad/s. This truncation of high-frequency components results in undercounting of level crossings. The undercount per unit time, denoted r, is a function of Δt as well as the frequency characteristics of the process. So, r is a function of Δt, ω_f and ζ_f. Approximate expressions for r are:

$$r(\tau) = 1 - 0.0005(\omega_f(\tau) + \zeta_f(\tau)) - 0.00425\omega_f(\tau)\zeta_f(\tau) \quad \text{when} \quad \Delta t = 0.01, \quad (14)$$

$$r(\tau) = 1 - 0.01\zeta_f(\tau) - 0.009\omega_f(\tau)\zeta_f(\tau) \quad \text{when} \quad \Delta t = 0.02. \quad (15)$$

Since digitally recorded accelerograms are available only in the discretized form, the count $N(0^+, t)$ underestimates the true number of crossings of the target accelerogram by the factor $r(\tau)$ per unit time. Hence, to account for this effect, we must multiply the rate of counted up-crossings by the factor $1/r(\tau)$. However, $r(\tau)$ depends on the predominant frequency and bandwidth of the accelerogram. So, it is more convenient to adjust the theoretical mean up-crossing rate [the first term inside the square brackets in Eq. (7)] by multiplying it by the factor $r(\tau)$. In order to solve Eq. (7), the filter damping ratio, ζ_f which controls the bandwidth of the process is selected. Corresponding ω_0 and ω_n are calculated. The value of ζ_f which best fits the target is chosen.

3. Simulation Model of Stochastic Ground Motion

A method to generate an ensemble of artificial earthquake ground motions is described in this section; based upon the stochastic ground motion model described in the previous section. A database of 100 recorded earthquake ground motions is created. In the next step, the nine parameters (six corresponding to modulating function, and three corresponding to the filter) required to depict a particular ground motion is found out for all the ground motions in the database. Probability distributions are created for the parameters of all the earthquakes in the database. Now, the parameters required by the stochastic ground motion model to simulate ground motions are obtained from the distributions. MC simulations are used to generate an ensemble of ground motions. A database of recorded earthquake accelerograms is created while the earthquakes are selected arbitrarily. Digital records of earthquakes with intensity varying from moderate to high that have occurred throughout the world in the past century are chosen from the United States Geological Survey (http://www.usgs.gov) website, and the exhaustive characteristics of the earthquakes in the database are available in Jacob [2010].

3.1. *Determination of parameters*

The nine parameters of the stochastic ground motion model are found out for each of the earthquakes in the database. The two additional parameters required are the time duration, T_n and the time steps, Δt. T_n is known from the time history and Δt taken for all the earthquakes from the database. The results are obtained and shown here for one accelerogram. The accelerogram chosen is the 90 component of October 18th, 1989 Loma Prieta earthquake recorded at Los Gatos Presentation Center. The six parameters required for the modulating function can be obtained by solving Eq. (6) using an optimization technique (Nelder–Mead simplex algorithm is used in the present study). Figure 1 compares the two energy terms $E_x(t) = (\frac{1}{2}) \int_0^t q^2(\tau, \boldsymbol{\alpha}) \mathrm{d}\tau$ and $E_a(t) = (\frac{1}{2}) \int_0^t a^2(\tau) \mathrm{d}\tau$.

It is seen that the fit is good at all the time points. Upon minimizing the error, the parameters after optimization, T_0, T_1, T_2, $\sigma_{\max}$, α, β obtained are 0.072932 s, 8.0154 s, 12.88 s, 0.16308 g, 0.80585 s^{-1}, 0.44846, respectively. Time duration of the ground motion is 25 s and time steps is 0.02 s. Using the same method of optimization, the parameters in the filter is obtained by solving Eq. (7). To solve this equation, first a value of ζ_f is assumed, which is considered to be constant for the entire duration of the earthquake. After obtaining the values of ω_0 and ω_n, separate optimization is done by minimizing the difference between the cumulative count of negative maxima and positive minima of the target and the model. The values of ω_0 and ω_n are kept unchanged as it is found that there is not much significant variation. Now, as the exact value of ζ_f is known, the values of ω_0 and ω_n are found

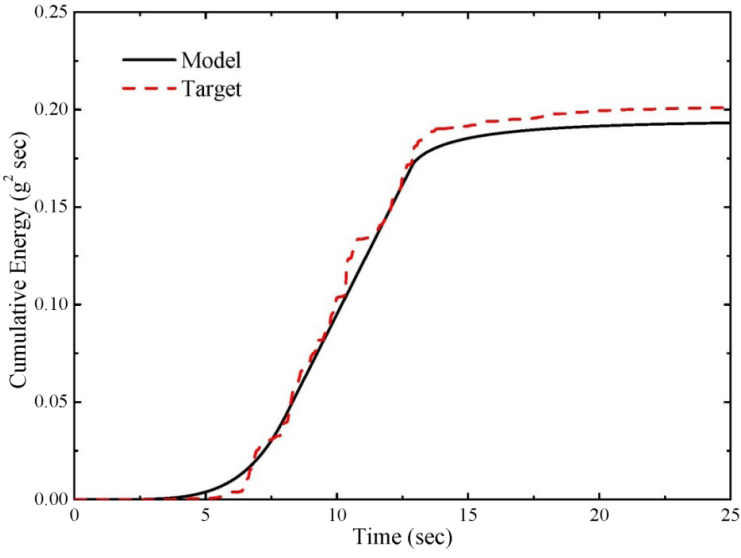

Fig. 1. (Color online) Cumulative energies in the target acceleration and the fitted model.

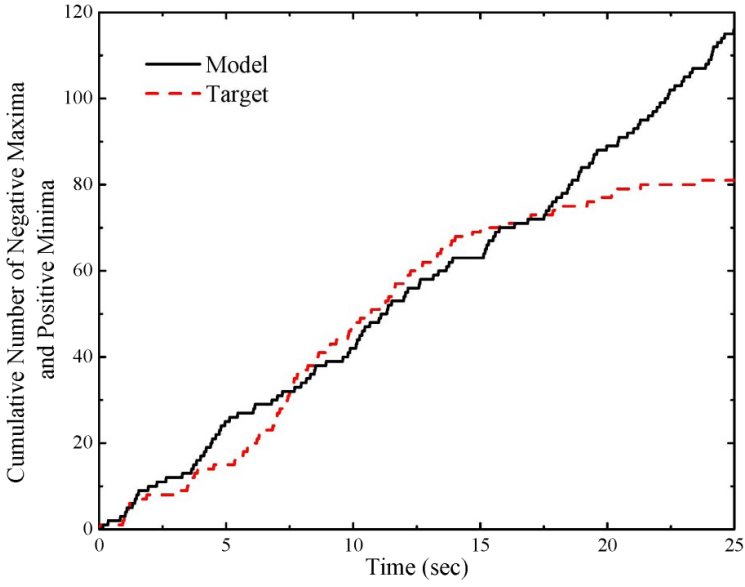

Fig. 2. (Color online) Cumulative count of negative maxima and positive minima.

corresponding to it. For the considered accelerogram it is found to be 0.8. Figure 2 shows the cumulative count of negative maxima and positive minima as a function of time for the Loma Prieta, 1989 record as well as the estimated values of the same quantity of the model with damping ratio, $\zeta_f = 0.8$. The slope of these lines should be considered as the instantaneous measure of bandwidth.

The parameters in the filter obtained after optimization for ω_0, ω_n and ζ_f are 30.297 rad/s, 10.075 rad/s and 0.8, respectively. In Fig. 3, the cumulative number of zero-level up-crossings as a function of time for the Loma Prieta, 1989 record as well as the estimated values of the same quantity of the model is shown.

It is seen that the fit is good at all the time points. The target accelerogram and a simulation are shown in Fig. 4.

3.2. *Parameter distributions*

After identifying the model parameter values by fitting to each recorded ground motion in the database, a probability distribution is assigned to the sample of values of each parameter. Now, there are 100 sets of parameters representing the 100 earthquakes with corresponding time steps, Δt. Distribution models are assigned to each of the 10 parameters. It is found that the data of all the 10 parameters are effectively fitted by β distribution. The statistical details of the data of each parameter are given in Table 1. Figure 5 shows the normalized frequency diagrams of the fitted model parameters for the entire dataset with the fitted probability density function (PDF) superimposed.

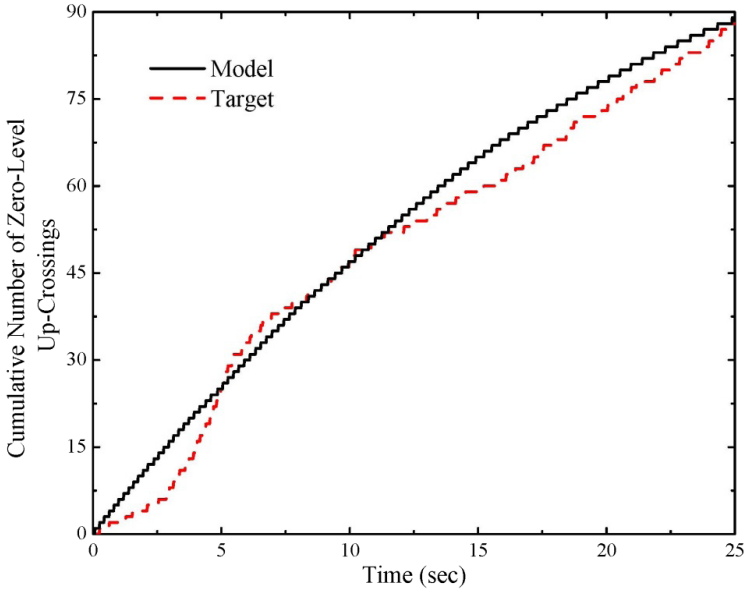

Fig. 3. (Color online) Cumulative number of zero-level up-crossings in the target accelerogram and model.

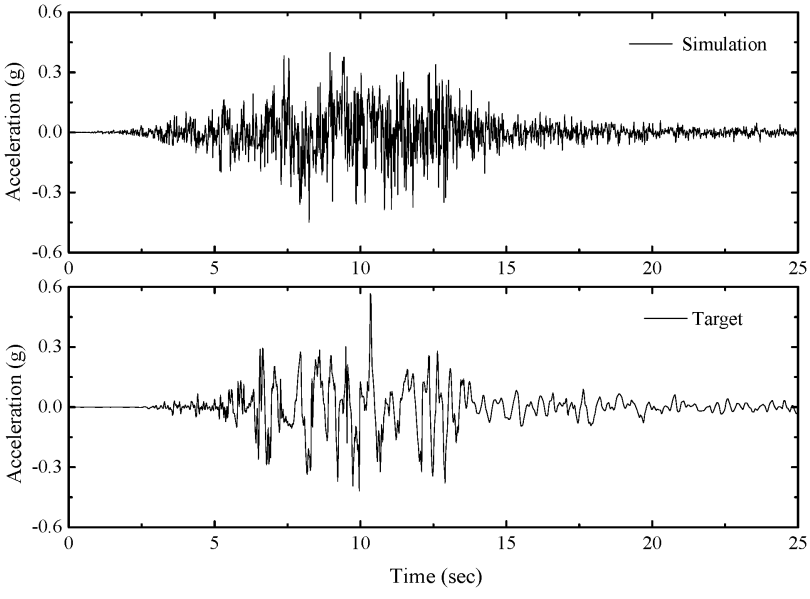

Fig. 4. Target accelerogram and a simulation using the fitted model.

Table 1. Statistical characteristics of parameters.

No.	Parameter	Mean	Standard deviation	Lowest value	Highest value
1	T_0	0.03	0.06	0.00	0.18
2	T_1	2.91	5.25	0.00	43.95
3	T_2	10.52	8.71	0.82	43.90
4	T_n	40.88	28.40	6.50	180.12
5	A	1.46	1.77	0.01	8.47
6	B	1.24	1.31	0.01	7.67
7	$\sigma_{\max}$	0.08	0.07	0.01	0.33
8	ω_0	31.89	13.28	8.86	73.26
9	ω_n	15.15	13.43	0.00	56.59
10	ζ_f	0.51	0.23	0.1	0.9

3.3. *Regenerating of ground motions*

A cluster of earthquake ground motions is reproduced by using the identified parameters. This is done by randomly selecting the parameters of the stochastic ground motion model. Initially, 10,000 samples of each parameter are arbitrarily chosen from the distributions of the particular parameter. From this pool of samples, 5000 sets of parameters which satisfy the conditions are chosen. Using these 5000 sets of parameters, 5000 artificial ground motions are generated. This cluster of earthquakes represents a completely random choice of ground motions.

4. Application to Stochastic Seismic Response of Base-Isolated Buildings

In this section, the proposed model is employed to study the stochastic seismic response of base-isolated buildings by using direct MC simulations. The uncertainty in the characteristics of the ground motion is considered and all the structural parameters are considered to be deterministic. Response analysis and parametric studies are presented below; the deterministic analysis is described elsewhere [Matsagar and Jangid, 2004; Jacob, 2010].

4.1. *Mathematical model*

Herein, lumped mass modeling is done for the superstructure and the isolator of a base-isolated building. The effect of rotation in the superstructure masses and isolator is not taken into consideration. The base-isolated building is modeled as a shear type structure mounted on isolation systems with one lateral degree-of-freedom at each floor. Figure 6 shows the idealized mathematical model of the five-storey base-isolated building considered for the present study.

The following assumptions are made for the structural system under consideration: (i) The superstructure is considered to remain within elastic limit during the earthquake excitation, owing mainly to the almost rigid superstructure behavior in base-isolated structures. (ii) The floors are assumed rigid in its own plane and

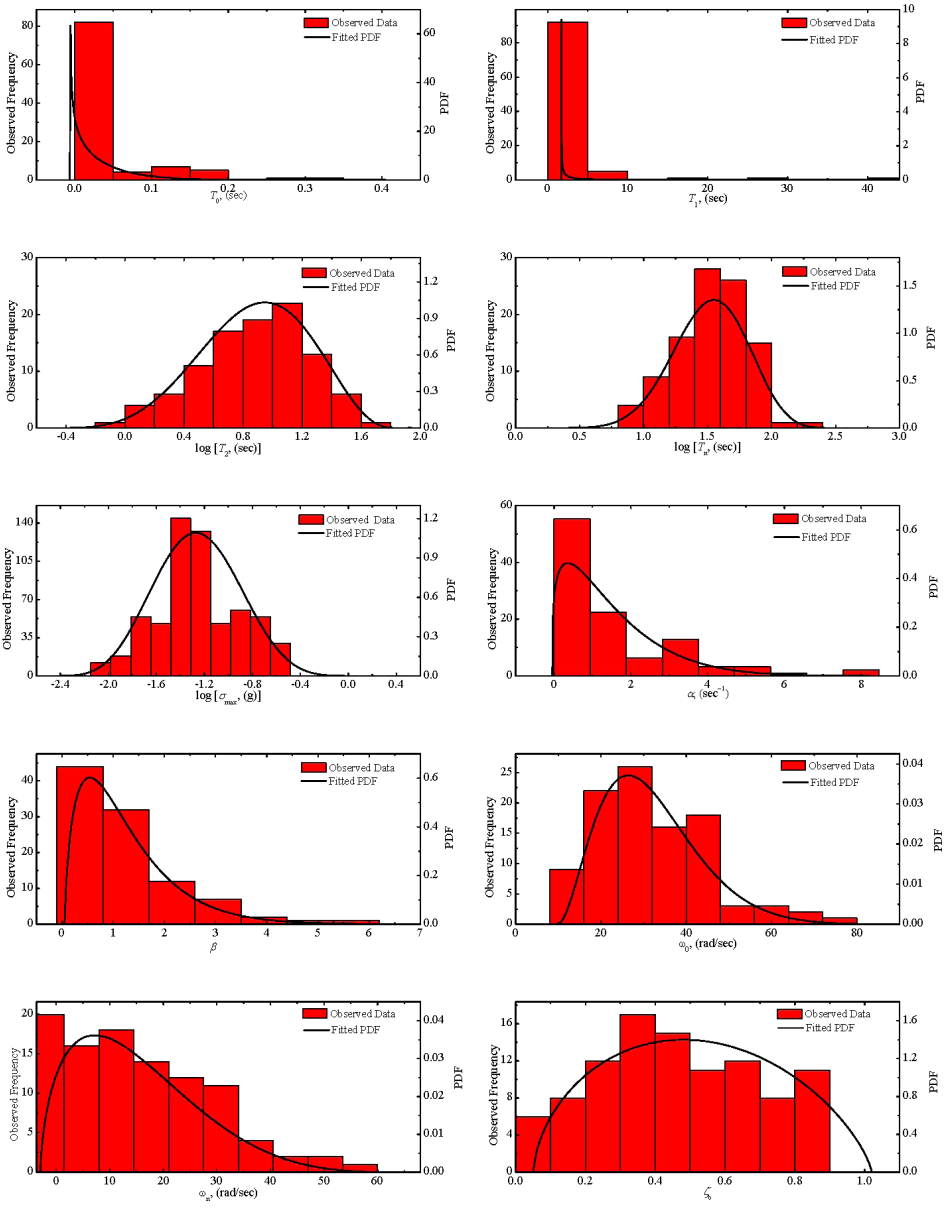

Fig. 5. (Color online) PDF of parameters superimposed on the observed normalized frequency (Hz).

the mass is supposed to be lumped at each floor level. (iii) The columns are inextensible and weightless providing the lateral stiffness. (iv) The system is subjected to single horizontal component of the earthquake ground motion. (v) The effect of soil-structure interaction is neglected. In Fig. 6, x_j is the relative floor displacement

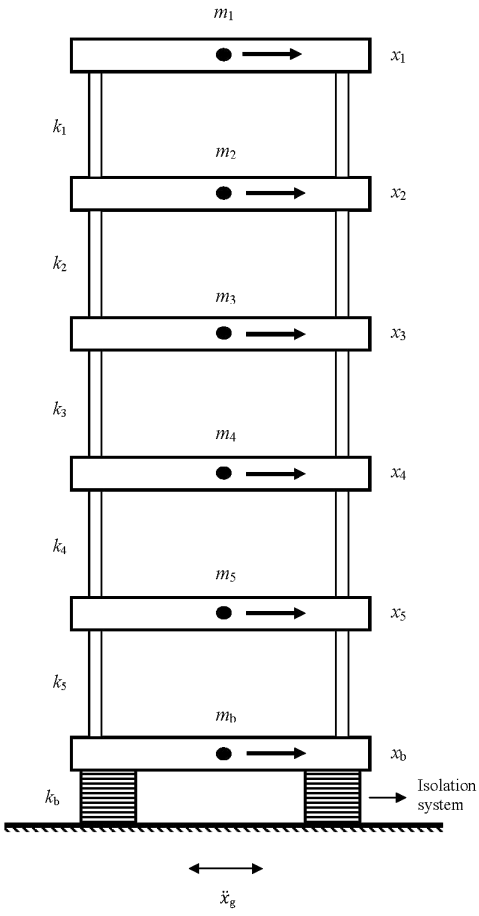

Fig. 6. Mathematical model of a five-storey base-isolated building.

at the jth-floor, m_j is the floor mass at the jth-floor, k_j is the stiffness of the jth-floor, x_b is the displacement at the isolator level, and m_b is the mass of the floor at isolator level.

For the present study, the force-deformation behavior of the isolator is modeled as nonlinear hysteretic represented by a bilinear model as shown in Fig. 7. The similar type of representation can be found in literature [Matsagar and Jangid, 2004]. The nonlinear force-deformation behavior of the isolation system is modeled through the bilinear hysteresis loop characterized by three parameters namely: (i) characteristic strength, Q; (ii) post-yield stiffness, i.e., isolation stiffness, k_b; and (iii) yield displacement, q. The bilinear behavior is selected because this model can be used for several isolation systems used in practice ranging from elastomeric to sliding systems, and earlier studies have delineated effects of such modeling [Matsagar and Jangid, 2004]. The characteristic strength, Q is related to the yield strength of the

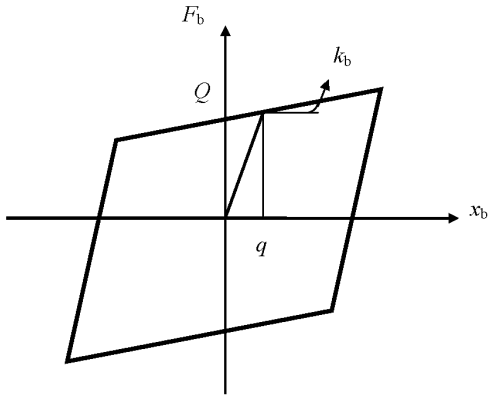

Fig. 7. Mathematical model of base isolator.

lead-core in the elastomeric bearings and friction coefficient of the sliding type isolation systems. The post-yield stiffness of the isolation system, k_b is generally designed in such a way to provide the specific value of the isolation period, T_b expressed as

$$T_b = 2\pi\sqrt{\frac{M}{k_b}}, \tag{16}$$

where $M = m_b + \sum_{j=1}^{5} m_j$ is the total mass of the base-isolated structure for a typical five-storey building. The characteristic strength, Q is mathematically related to the damping ratio, ζ_b by the following equation [Naeim and Kelly, 1999]

$$\zeta_b = \frac{4Q(D-q)}{2\pi k_b D^2}, \tag{17}$$

where D is the design displacement. Thus, the bilinear hysteretic model of the base isolation systems can be characterized by specifying the three parameters namely, T_b, Q and q. Further, the deterministic analysis has been elaborated by Matsagar and Jangid [2004] for a similar model.

4.2. *Response quantities*

The response quantities of interest are the absolute peak value of the acceleration at the top floor, hereinafter simply referred as top floor acceleration and the peak value of the isolator displacement hereinafter simply referred as isolator displacement. To perform the response analysis, a total of 5000 artificial earthquakes are simulated as described earlier. Deterministic analysis is performed for each simulation and their corresponding response quantities are calculated. The deterministic results are then processed to find the peak values, RMS values and distributions of the response quantities. While calculating the responses, the parameters of the structure are kept unchanged. The input parameters are considered as the superstructure time period (0.5 s), damping of the superstructure (taken as 0.02 for all the modes of

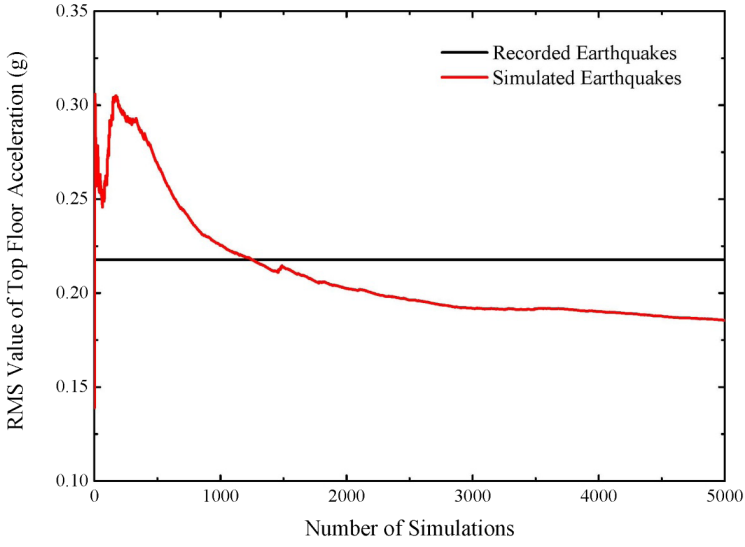

Fig. 8. (Color online) RMS value of top floor acceleration for recorded and simulated earthquakes.

vibration) and the mass and stiffness of the each floor. The mass of each floor is kept constant, while the stiffness is varied from 1 at lowest floor to 3 at top floor with an increment of 0.5 at each floor level. The mass of the isolator is considered to be equal to that of a floor. Here, it can be mentioned that the mass and stiffness of each floor have been taken in such a ratio that the specified superstructure time period is achieved. The damping ratio of the isolator, ζ_b is 0.1. The time period of the isolator, T_b is taken as 2 s. The design displacement, D is taken as 40 cm and yield displacement, q is taken as 2.5 cm. A comparison of RMS values of the peak top floor acceleration of the structure is shown between the actual recorded earthquakes and earthquakes simulated by using the model is shown in Fig. 8. It confirms that there is a convergence when the number of simulations is higher. The distributions of the responses are calculated. The top floor acceleration is found to be fitted effectively by using beta distribution and the isolator displacement is effectively fitted by generalized Pareto distribution. The PDFs of the response quantities are plotted and superimposed with their observed frequency diagrams as shown in Fig. 9.

The cumulative distribution function (CDF) is plotted for both the response quantities and is shown in Fig. 10. For the considered parameters, the extreme top floor acceleration is found to be $0.89\,g$ and the extreme isolator displacement is found to be 92 cm. Their corresponding RMS values are $0.185g$ and 9.122 cm. An attempt is made to study the characteristics of the earthquakes which produce extreme responses. After 5000 simulations, 40 earthquakes were found to produce top floor acceleration in excess of $0.4g$ and 38 earthquakes were found to produce an isolator displacement in excess of 40 cm. It is seen that the base isolation is effective

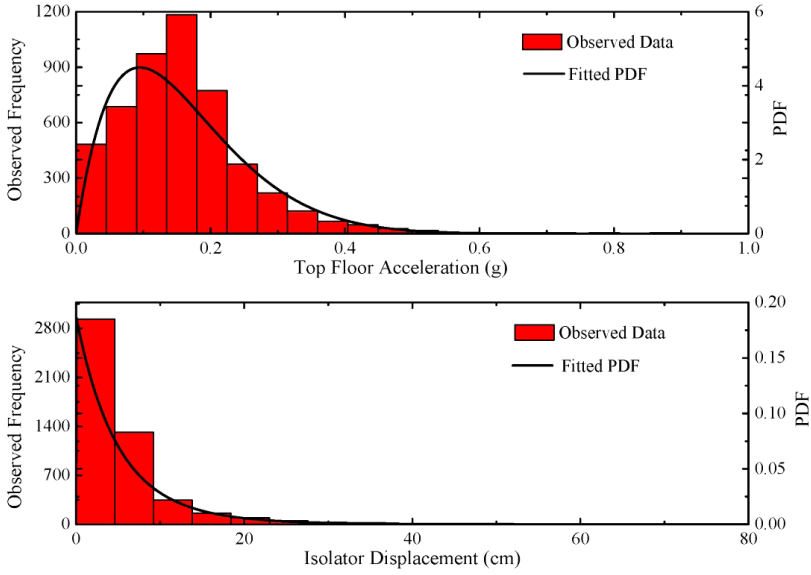

Fig. 9. (Color online) PDF of response quantities superimposed on observed normalized frequency (Hz).

for more than 99% of the earthquakes generated. After studying the parameters of the earthquakes that produce extreme responses, it is found that most of the earthquakes have a high value of RMS ground acceleration in the strong motion phase which is given by the parameter, $\sigma_{\max}$. However, there are some earthquakes with lesser value of $\sigma_{\max}$ which produce higher responses. This is due to the fact that the predominant frequency of the earthquake ground motion approaches the fundamental frequency of the base-isolated building considered which induces the phenomenon of resonance. To establish a relationship between the characteristics of these earthquakes and for a detailed study of these extreme earthquakes a huge number of simulations are required.

4.3. *Probability of failure*

The probability of failure or limit state probability for this system is defined using a limit state function, which is defined as the case where the top floor accelerations reach a $0.3g$ acceleration level. This can be formally stated with the limit state function as $h(X) = 0.3 - a_i$, where a_i is the peak acceleration of the top floor in g. Then, the probability of failure is defined as:

$$P_f = P[h(X) \leq 0]. \tag{18}$$

The probability of failure is evaluated via MC simulation by determining the number of realizations with $h(X) < 0$ and dividing that number by the total number of simulations. The convergence of the probability of failure is demonstrated in

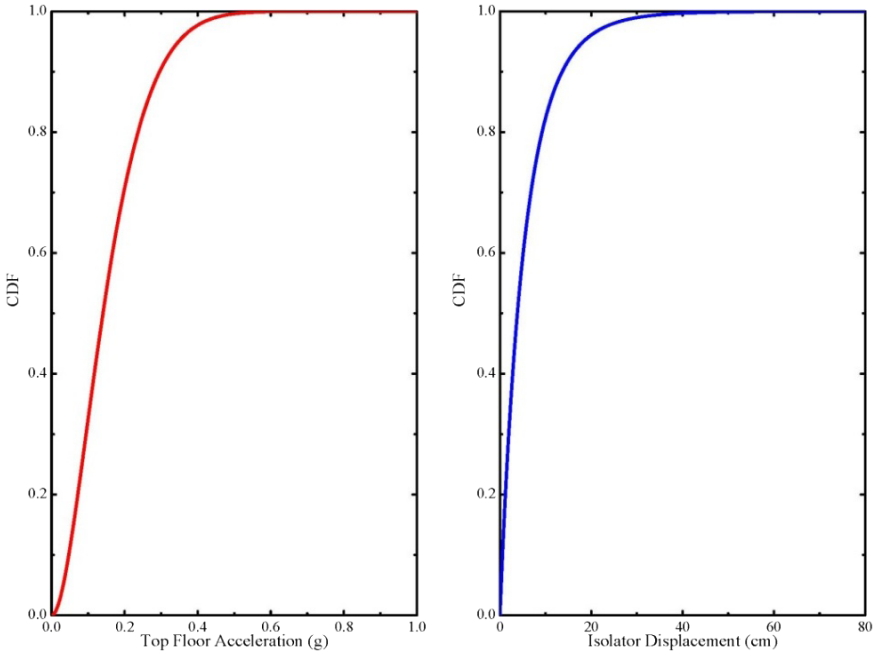

Fig. 10. (Color online) CDF of response quantities.

Fig. 11 where the isolator parameters taken are, $T_b = 2\,\text{s}$, $q = 2.5\,\text{cm}$, $\zeta_b = 0.1$ and $D = 40\,\text{cm}$. From Fig. 11, it is seen that the probability of failure reaches a constant level at around 5000 simulations. Therefore, the convergence is achieved after 5000 simulations.

4.4. *Parametric studies*

Analyses are conducted for different isolation time periods (T_b) and isolation damping ratios (ζ_b). Combinations of isolation periods of 2, 3, 4 and 5 s, isolation damping ratios of 5, 10, 15 and 20% and isolator yield displacements of 0.01, 2.5 and 5 cm are considered. Therefore, a total of 64 different structures are analyzed. For every combination, the design displacement, D of the isolator is kept constant at 40 cm. The peak top floor acceleration and peak isolator displacement, and RMS values corresponding to these are shown in Tables 2–5. The RMS values of the response quantities for 200 simulations as shown in Table 3 and the corresponding values for 400 simulations shown in Table 5 are not varying significantly. So, the number of simulations for conducting parametric studies is fixed at 400.

It is observed that the top floor acceleration decreases with the increase in the yield displacement of the isolator and the isolator displacement decreases with the increase in the yield displacement.

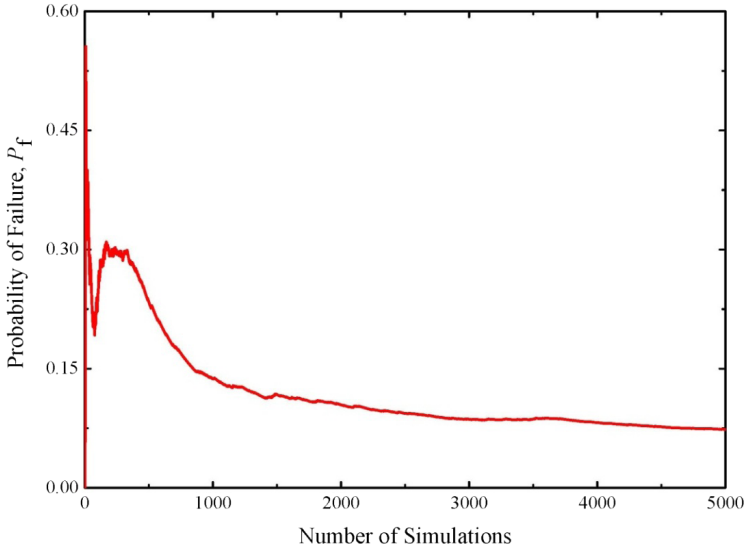

Fig. 11. (Color online) An example of convergence of probability of failure of the structure for the selected isolation system.

Table 2. Peak values of the response of the structure: 200 simulations.

Parameters	Top floor acceleration (g)				Isolator displacement (cm)			
	$\zeta_b = 0.05$	$\zeta_b = 0.1$	$\zeta_b = 0.15$	$\zeta_b = 0.2$	$\zeta_b = 0.05$	$\zeta_b = 0.1$	$\zeta_b = 0.15$	$\zeta_b = 0.2$
$T_b = 2\,\text{s}$								
$q = 0.01\,\text{cm}$	0.93	1.03	1.2	1.41	83.28	65.54	46.4	44.47
$q = 2.5\,\text{cm}$	1	0.9	1.08	1.19	85.94	67.33	49.53	45.47
$q = 5\,\text{cm}$	1	0.87	0.9	1.06	86.79	69.25	55.1	45.54
$T_b = 3\,\text{s}$								
$q = 0.01\,\text{cm}$	0.92	0.68	0.73	0.77	211.77	152.85	130.88	116.13
$q = 2.5\,\text{cm}$	0.92	0.7	0.6	0.61	210.52	158.47	136.64	122.41
$q = 5\,\text{cm}$	0.9	0.7	0.58	0.51	203.82	162.15	140.13	127.05
$T_b = 4\,\text{s}$								
$q = 0.01\,\text{cm}$	0.82	0.63	0.55	0.52	339.29	284.78	247.1	217.39
$q = 2.5\,\text{cm}$	0.82	0.62	0.52	0.45	336.75	281.76	243.81	217.2
$q = 5\,\text{cm}$	0.79	0.63	0.51	0.42	332.92	284.08	241.39	222.21
$T_b = 5\,\text{s}$								
$q = 0.01\,\text{cm}$	0.92	0.81	0.78	0.6	600.32	561.73	585.86	506.79
$q = 2.5\,\text{cm}$	0.9	0.78	0.74	0.6	596.43	563.25	572.98	489.96
$q = 5\,\text{cm}$	0.88	0.8	0.7	0.52	590.34	571.18	557.81	466

Figure 12 shows the variation of response quantities for different isolation periods T_b and isolation damping ratios ζ_b, the value of the yield displacement of the isolator q is assumed as 2.5 cm. It can be seen that the top floor acceleration decreases as the isolation time period increases. Also, the top floor acceleration decreases as the damping ratio increases. The displacement in the isolator increases as the time

Table 3. RMS values of the response of the structure: 200 simulations.

Parameters	Top floor acceleration (g)				Isolator displacement (cm)			
	$\zeta_b = 0.05$	$\zeta_b = 0.1$	$\zeta_b = 0.15$	$\zeta_b = 0.2$	$\zeta_b = 0.05$	$\zeta_b = 0.1$	$\zeta_b = 0.15$	$\zeta_b = 0.2$
$T_b = 2\,\mathrm{s}$								
$q = 0.01\,\mathrm{cm}$	0.35	0.49	0.6	0.7	19.74	13.03	9.92	8.51
$q = 2.5\,\mathrm{cm}$	0.28	0.3	0.38	0.47	21.53	14.72	12.16	10.58
$q = 5\,\mathrm{cm}$	0.29	0.28	0.32	0.37	23.12	16.65	13.96	12.57
$T_b = 3\,\mathrm{s}$								
$q = 0.01\,\mathrm{cm}$	0.25	0.29	0.37	0.43	44.98	34.12	27.58	24.24
$q = 2.5\,\mathrm{cm}$	0.22	0.19	0.19	0.21	45.94	35.51	29.82	26.67
$q = 5\,\mathrm{cm}$	0.22	0.18	0.17	0.18	46.45	36.64	31.11	28.28
$T_b = 4\,\mathrm{s}$								
$q = 0.01\,\mathrm{cm}$	0.2	0.21	0.26	0.3	71.09	58.19	50.76	47.14
$q = 2.5\,\mathrm{cm}$	0.18	0.15	0.14	0.14	71.67	58.68	52	49.04
$q = 5\,\mathrm{cm}$	0.18	0.15	0.13	0.13	71.9	59.02	52.95	50.55
$T_b = 5\,\mathrm{s}$								
$q = 0.01\,\mathrm{cm}$	0.17	0.18	0.2	0.23	99.58	92.66	88.35	81.46
$q = 2.5\,\mathrm{cm}$	0.16	0.14	0.13	0.12	99.44	92.9	88.56	82.48
$q = 5\,\mathrm{cm}$	0.15	0.14	0.12	0.11	99.31	93.3	88.5	82.67

Table 4. Peak values of the response of the structure: 400 simulations.

Parameters	Top floor acceleration (g)				Isolator displacement (cm)			
	$\zeta_b = 0.05$	$\zeta_b = 0.1$	$\zeta_b = 0.15$	$\zeta_b = 0.2$	$\zeta_b = 0.05$	$\zeta_b = 0.1$	$\zeta_b = 0.15$	$\zeta_b = 0.2$
$T_b = 2\,\mathrm{s}$								
$q = 0.01\,\mathrm{cm}$	0.99	1.03	1.25	1.59	85.76	67.94	54.44	44.71
$q = 2.5\,\mathrm{cm}$	1	0.9	1.08	1.27	87.79	75.98	61.18	45.47
$q = 5\,\mathrm{cm}$	1	0.92	0.9	1.06	87.49	75.36	65.62	49.34
$T_b = 3\,\mathrm{s}$								
$q = 0.01\,\mathrm{cm}$	0.92	0.68	0.73	0.77	211.77	152.85	130.88	116.13
$q = 2.5\,\mathrm{cm}$	0.92	0.7	0.6	0.61	210.52	158.47	136.64	122.41
$q = 5\,\mathrm{cm}$	0.9	0.7	0.58	0.51	203.82	162.15	140.13	127.05
$T_b = 4\,\mathrm{s}$								
$q = 0.01\,\mathrm{cm}$	0.82	0.71	0.57	0.57	339.29	314.27	267.91	217.39
$q = 2.5\,\mathrm{cm}$	0.83	0.7	0.58	0.45	337.17	317.72	266.66	217.2
$q = 5\,\mathrm{cm}$	0.83	0.7	0.51	0.43	340.3	314.89	258.74	222.21
$T_b = 5\,\mathrm{s}$								
$q = 0.01\,\mathrm{cm}$	0.92	0.81	0.78	0.6	600.32	561.73	585.86	506.79
$q = 2.5\,\mathrm{cm}$	0.9	0.78	0.74	0.6	596.43	563.25	572.98	489.96
$q = 5\,\mathrm{cm}$	0.88	0.8	0.7	0.52	590.34	571.18	557.81	466

period increases, and decreases as the damping ratio increase. The acceleration response decreases with increasing isolation time periods (lowest for the selected $T_b = 5\,\mathrm{s}$). However, peak isolator displacement is high corresponding to long isolation time periods. This problem can be solved by employing high damping in the isolators. Therefore, the isolation system with a long isolation time period and high damping is the most effective. This design approach for the isolation system can help design engineers in designing reliable isolation systems.

Table 5. RMS values of the response of the structure: 400 simulations.

Parameters	Top floor acceleration (g)				Isolator displacement (cm)			
	$\zeta_b = 0.05$	$\zeta_b = 0.1$	$\zeta_b = 0.15$	$\zeta_b = 0.2$	$\zeta_b = 0.05$	$\zeta_b = 0.1$	$\zeta_b = 0.15$	$\zeta_b = 0.2$
$T_b = 2\,\mathrm{s}$								
$q = 0.01\,\mathrm{cm}$	0.33	0.47	0.58	0.67	17.97	11.74	8.97	7.63
$q = 2.5\,\mathrm{cm}$	0.26	0.28	0.37	0.45	19.64	13.65	11.31	9.7
$q = 5\,\mathrm{cm}$	0.27	0.27	0.3	0.35	21.12	15.57	13.2	11.61
$T_b = 3\,\mathrm{s}$								
$q = 0.01\,\mathrm{cm}$	0.23	0.28	0.35	0.42	40.9	30.05	23.88	20.6
$q = 2.5\,\mathrm{cm}$	0.2	0.17	0.18	0.2	41.73	31.5	25.92	22.99
$q = 5\,\mathrm{cm}$	0.2	0.17	0.16	0.17	42.24	32.66	27.23	24.63
$T_b = 4\,\mathrm{s}$								
$q = 0.01\,\mathrm{cm}$	0.18	0.21	0.25	0.29	65.58	53.73	45.62	40.69
$q = 2.5\,\mathrm{cm}$	0.17	0.14	0.13	0.13	66.02	54.33	46.82	42.48
$q = 5\,\mathrm{cm}$	0.17	0.14	0.12	0.12	66.33	54.7	47.69	43.94
$T_b = 5\,\mathrm{s}$								
$q = 0.01\,\mathrm{cm}$	0.15	0.16	0.19	0.22	89.8	82.49	75.56	67.96
$q = 2.5$ cm	0.14	0.12	0.11	0.1	89.88	82.67	75.9	69.2
$q = 5\,\mathrm{cm}$	0.14	0.12	0.11	0.1	89.92	82.91	75.92	69.6

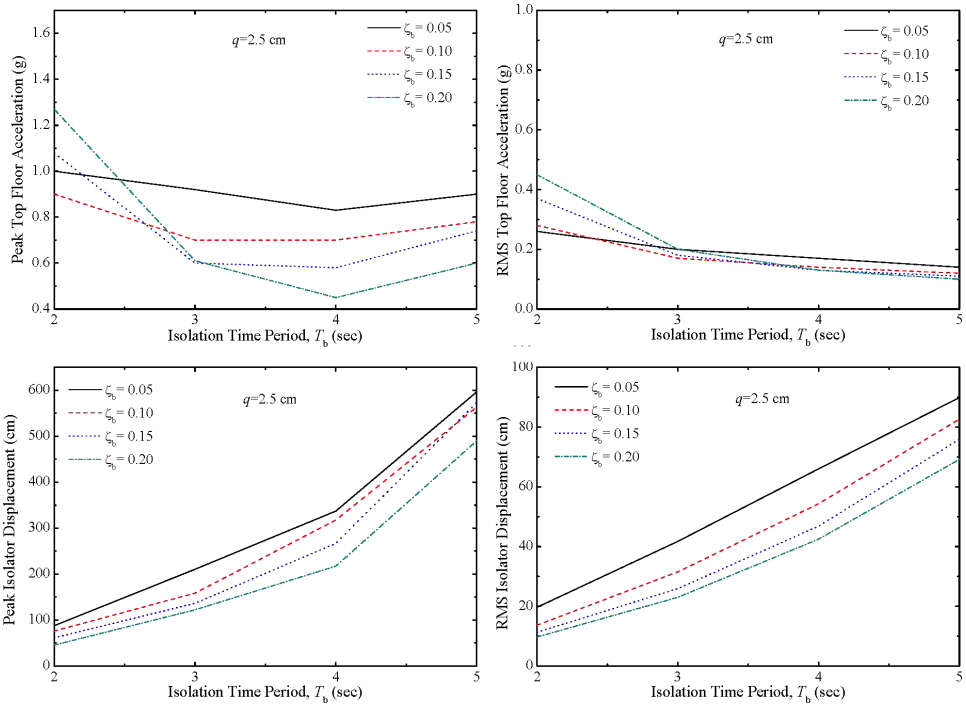

Fig. 12. (Color online) Variation of response quantities for different isolation periods and isolation damping ratios, for $q = 2.5\,\mathrm{cm}$ and 400 simulations.

5. Summary and Conclusions

The stochastic response of base-isolated building considering the uncertainty in the characteristics of the earthquakes is investigated. In this study, a database of recorded earthquakes is created and a probabilistic method to generate artificial earthquakes based on recorded ground motions in the database is provided. Using MC simulations, the stochastic response of a five-storey base-isolated building under earthquake excitations is reported by considering the earthquake parameters to be uncertain. A study on the parameters of the earthquake which produces very high responses is attempted. A parametric study based on the isolator characteristics is done. Based on the study reported herein it is concluded that about 0.8% of the earthquakes simulated by using the probabilistic model produces very high responses. These earthquakes generally have very high average intensity in the strong motion phase. Moreover, it is also concluded that the isolation system with a long isolation period and high damping is the most effective as demonstrated through the simulation.

References

Alhan, C. and Gavin, H. P. [2005] "Reliability of base isolation for the protection of critical equipment from earthquake hazards," *Engineering Structures* **27**, 1435–1449.

Buckle, I. G. and Mayes, R. L. [1990] "Seismic isolation history, application and performance — A world review," *Earthquake Spectra* **6**, 161–202.

Constantinou, M. C. and Papageorgiou, A. S. [1990] "Stochastic response of practical sliding isolation systems," *Probabilistic Engineering Mechanics* **5**, 27–34.

Conte, J. P. and Peng, B. F. [1997] "Fully non-stationary analytical earthquake ground-motion model," *Journal of Engineering Mechanics (ASCE)* **12**, 15–24.

Er, G. K. and Iu, V. P. [2000] "Stochastic response of base-excited Coulomb oscillator," *Journal of Sound and Vibration* **233**, 81–92.

Fan, F. G. and Ahmadi, G. [1990] "Nonstationary Kanai–Tajimi models for El Centro 1940 and Mexico City 1985 earthquakes," *Probabilistic Engineering Mechanics* **5**(4), 171–181.

Housner, G. W. and Jennings, P. C. [1964] "Generation of artificial earthquakes," *Journal of Engineering Mechanics (ASCE)* **90**, 113–150.

Ibrahim, R. A. [2008] "Recent advances in nonlinear passive vibration isolators," *Journal of Sound and Vibration* **314**(3–5), 371–452.

Jacob, C. M. [2010] "Stochastic response of isolated structures under earthquake excitation," Masters Dissertation, Indian Institute of Technology (IIT) Delhi, India.

Jangid, R. S. and Datta, T. K. [1995] "Seismic behavior of base-isolated buildings: A state-of-the-art review," *Structures and Buildings* **110**(2), 186–203.

Jensen, H. and Iwan, W. D. [1992] "Response of systems with uncertain parameters to stochastic excitation," *Journal of Engineering Mechanics, American Society of Civil Engineers (ASCE)* **118**(5), 1012–1026.

Jensen, H., Sepulveda, J. and Becerra, L. [2012] "Robust stochastic design of base-isolated structural systems," *International Journal of Uncertainty Quantification* **2**(2), 95–110.

Kelly, J. M. [1986] "A seismic base isolation: Review and bibliography," *Soil Dynamics and Earthquake Engineering* **5**(4), 202–216.

Kiureghian, A. D. and Crempien, J. [1989] "An evolutionary model for earthquake ground motion," *Structural Safety* **6**, 235–246.

Matsagar, V. A. and Jangid, R. S. [2004] "Influence of isolator characteristics on the response of base-isolated structures," *Engineering Structures* **26**(12), 1735–1749.

Naeim, F. and Kelly, J. M. [1999] *Design of Isolated Structures, From Theory to Practice* (John Wiley and Sons, New York, USA).

Rezaeian, S. and Kiureghian, A. D. [2008] "A stochastic ground motion model with separable temporal and spectral non-stationarities," *Earthquake Engineering and Structural Dynamics* **37**, 1565–1584.

Schueller, G. I., Pradlwarter, H. J. and Dorka, U. [1988] "Reliability of MDOF-systems with hysteretic devices," *Engineering Structures* **20**(8), 685–691.

Sepahvand, K., Marburg, S. and Hardtke, H.-J. [2011] "Stochastic structural modal analysis involving uncertain parameters using generalized polynomial chaos expansion," *International Journal of Applied Mechanics* **3**(3), 587–606.

Shinozuka, M. and Deodatis, G. [1988] "Stochastic process models for earthquake ground motion," *Probabilistic Engineering Mechanics* **3**, 114–123.

Su, L. and Ahmadi, G. [1988] "Response of frictional base isolation systems to horizontal–vertical random earthquake excitations," *Probabilistic Engineering Mechanics* **3**(1), 12–21.

Yeh, C. H. and Wen, Y. K. [1990] "Modeling of non-stationary ground motion and analysis of inelastic structural response," *Structural Safety* **8**, 281–298.

Zerva, A. [1988] "Seismic source mechanisms and ground motion models, review paper," *Probabilistic Engineering Mechanics* **3**, 64–74.